J Electroceram (2010) 24:326–330
DOI 10.1007/s10832-009-9578-7

Electrical and structural properties of Nb-doped $SrTiO_3$ ceramics

J. Karczewski · B. Riegel · M. Gazda · P. Jasinski · B. Kusz

Received: 27 January 2009 / Accepted: 6 May 2009 / Published online: 20 May 2009
© Springer Science + Business Media, LLC 2009

Abstract Niobium-doped strontium titanate synthesized via conventional solid-state reaction has been studied. Influence of niobium content on the lattice parameters and electrical conductivity has been reported. Various reduction conditions have been investigated. For samples reduced in hydrogen at 1400°C, a transition from thermally activated to metallic behavior has been observed. Maximum electrical conductivity (ca. 55 Scm^{-1} at 650°C) has been observed for the $SrTi_{0.98}Nb_{0.02}O_{3-\delta}$ sample. The relation of electrical conductivity with the porosity of the samples has been shown.

Keywords Electrical conductivity · Nb-doped Strontium titanate · Anode materials · Solid oxide fuel cell

1 Introduction

The NiO and yttria-stabilized zirconia (YSZ) cermet (Ni-YSZ) commercially used as an anode material for solid oxide fuel cells (SOFC) suffers some fundamental limitations. It seems to be necessary to discover a new anode material overcoming the disadvantages of Ni-YSZ. Fergus has compared a variety of the oxide anode materials [1]. Perovskites based on the strontium titanate seem to be one of the most competitive choices. They can be used as an anode material for solid oxide fuel cells (SOFC) working at high as well as at intermediate temperatures. Such perovskite materials present a very good stability over working cycles in various atmospheres [2, 3], have large triple phase boundary [2, 4] and are chemically and thermally compatible with the electrolyte [2–5]. Moreover, they eliminate some fundamental problems of cermet anodes: deposition of carbon when using hydrocarbon fuels and poisoning by sulphur [2, 6, 7].

The $SrTiO_3$ is an example of the perovskite family of general formula ABO_3. Its total electrical conductivity can be increased by doping a rare earth element into the A sublattice or a transition metal into the B sublattice [8–10]. Doped strontium titanates have been investigated since early 1980's, although most of the oldest works deal with the lanthanum doping [11–15]. Later, the yttrium addition to the pure strontium titanate and the deficiency on the strontium site has been examined [7, 8, 16, 17]. Recently, the attention has been paid again to the niobium doping into the B sublattice [18–21], where Nb^{5+} substitutes Ti^{4+}, bringing more oxide ions or more electrons into the system. Niobium-doped samples have several significantly improved properties [8, 16, 18–20], depending on where the oxygen incorporates in the structure and to which extent the extra charge of Nb^{5+} is compensated. Either the cation vacancies are created in order to fulfill the electroneutrality condition or there must be excessive oxygen ions occupying the interstitial oxygen positions in perovskites. It is reported that probably the strontium vacancies are predominant defects in the donor-doped $SrTiO_3$ [22]. For equal number of A-site and B-site cations in ABO_3 the effect would be a creation of a strontium oxide phase. According to the Kröger-Vink notation it can be written, that if

J. Karczewski (✉) · B. Riegel · M. Gazda · B. Kusz
Faculty of Applied Physics and Mathematics,
Gdansk University of Technology,
Gdansk, Poland
e-mail: ja_kubek@wp.pl

P. Jasinski
Faculty of Electronics, Telecommunications and Informatics,
Gdansk University of Technology,
Gdansk, Poland

strontium vacancies are the preferred species, the incorporation reaction will be as followed [18]:

$$\mathrm{SrO} + (1-\mathrm{x})\mathrm{TiO_2} + (\mathrm{x}/2)\mathrm{Nb_2O_5} \rightarrow (1-\mathrm{x}/2)\mathrm{Sr}^{\mathrm{x}}_{\mathrm{Sr}} + (\mathrm{x}/2)\mathrm{V}''_{\mathrm{Sr}} + (1-\mathrm{x})\mathrm{Ti}^{\mathrm{x}}_{\mathrm{Ti}} + \mathrm{xNb}^{\mathrm{o}}_{\mathrm{Ti}} + 3\mathrm{O}^{\mathrm{x}}_{\mathrm{o}} + (\mathrm{x}/2)\mathrm{SrO} \quad (1)$$

It means that in this case substituting x Ti atoms with Nb causes a creation of x/2 strontium vacancies. Simultaneously, x/2 of SrO is formed. The presence of strontium vacancies and the SrO phase enables the reduction of titanium and niobium, according to the (2) and (3) reactions:

$$\mathrm{SrO} + \mathrm{V}''_{\mathrm{Sr}} + 2\mathrm{Ti}^{\mathrm{x}}_{\mathrm{Ti}} \leftrightarrow 2\mathrm{Ti}'_{\mathrm{Ti}} + \mathrm{Sr}^{\mathrm{x}}_{\mathrm{Sr}} + 1/2\mathrm{O_2} \quad (2)$$

$$\mathrm{SrO} + \mathrm{V}''_{\mathrm{Sr}} + 2\mathrm{Nb}^{\mathrm{o}}_{\mathrm{Ti}} \leftrightarrow 2\mathrm{Nb}^{\mathrm{x}}_{\mathrm{Ti}} + \mathrm{Sr}^{\mathrm{x}}_{\mathrm{Sr}} + 1/2\mathrm{O_2} \quad (3)$$

Annealing of the Nb-doped $SrTiO_3$ ceramics in a reducing atmosphere influences its properties. For instance, Ferreira et al. reported that the reduction of strontium titanate causes its weight losses. It was interpreted as being caused by a change in charge compensation [23]. Moreover, Irvine et al. found that the reduction causes an increase in the lattice parameter of $Sr_{1-y/2}Ti_{1-y}Nb_yO_{3-\delta}$ materials (at 930°C). The authors explained it as a result of the reduction of Ti^{4+} to Ti^{3+} or Nb^{5+} to Nb^{4+} [24].

The aim of this work was to study the influence of Nb doping on the properties of strontium titanate. The effects of Nb amount on the electrical properties and unit cell parameters were investigated.

2 Experimental

$SrTi_{1-x}Nb_xO_{3-\delta}$ (x=0, 0.01, 0.02, 0.03, 0.06, 0.08) and $Sr_{1.01}Ti_{0.98}Nb_{0.02}O_{3-\delta}$ ceramics were prepared with conventional solid state reaction technique. Starting with $SrCO_3$, TiO_2, Nb_2O_5 the powders were mixed in a proper molar ratio, pressed into bars and calcinated in air at 1200°C for 12 h. Then, the pellets were milled, uniaxially pressed at 100 kN/cm^2 and sintered at 1400°C for 12 h in air. To obtain porous $SrTi_{1-x}Nb_xO_{3-\delta}$ samples the powder was mixed with starch (2–10 wt. %), pressed into the bars at 10 MPa and fired at 1400°C for 12 h with a heating rate of 1°Cmin^{-1}. After the synthesis samples were reduced in humidified hydrogen in various thermal conditions. The average thickness of samples was 1 mm. The phase composition was determined by X-ray diffraction (XRD) using Cu Kα (1.542Å) radiation at room temperature. The density of samples was measured with the Archimedes method.

The electrical conductivity was measured in humidified hydrogen by a standard four-terminal DC method. The measurements were taken with constant rate of heating and cooling. To ensure that the measurements were performed in equilibrium conditions, it was found that the results obtained in this way were identical with those taken after holding at each temperature for 30 min.

3 Results and discussion

All the $SrTi_{1-x}Nb_xO_{3-\delta}$ and $Sr_{1.01}Ti_{0.98}Nb_{0.02}O_{3-\delta}$ powders sintered in air and reduced in hydrogen were examined by XRD to identify their phase composition. The samples with x up to 0.03 show single cubic perovskite structure and no impurity phases were detected. The $SrTi_{0.94}Nb_{0.06}O_{3-\delta}$, $SrTi_{0.92}Nb_{0.08}O_{3-\delta}$, and $Sr_{1.01}Ti_{0.98}Nb_{0.02}O_{3-\delta}$ samples contain a trace amount of an impurity phase, which was identified as the Sr_2NbO_4. Typical XRD patterns of $SrTi_{0.98}Nb_{0.02}O_{3-\delta}$ and $Sr_{1.01}Ti_{0.98}Nb_{0.02}O_{3-\delta}$ are shown in Fig. 1. The unit cell parameters of the studied samples were determined by the Rietveld refining method. As shown in Table 1 the unit cell parameters of reduced samples are higher than these of non reduced samples. It suggests the presence of the reduced Ti^{3+} and Nb^{4+} ions, which ionic radius is bigger than the ionic radius of Ti^{4+} and Nb^{5+}. It causes the expansion of the cell. On the other hand, the results show that the increase of niobium content in $SrTi_{1-x}Nb_xO_{3-\delta}$ is not correlated with the unit cell parameter by a linear plot, as it is suggested by Blennow et al. [18]. It was observed that a maximum value of the unit cell parameter occurs for x=0.02. We think that for a small niobium

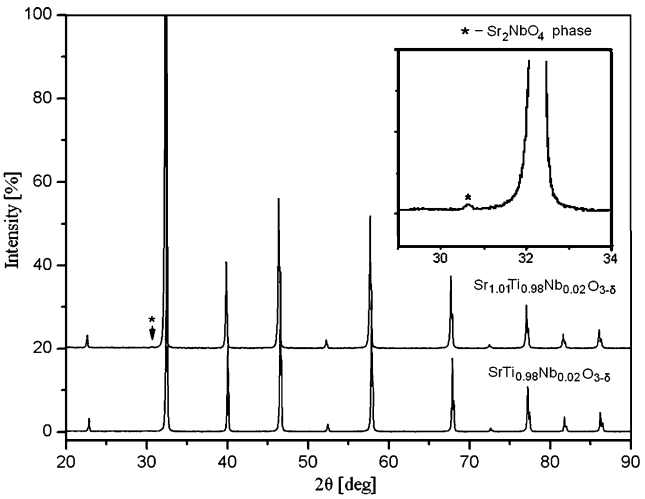

Fig. 1 XRD pattern of $SrTi_{0.98}Nb_{0.02}O_{3-\delta}$ and $Sr_{1.01}Ti_{0.98}Nb_{0.02}O_{3-\delta}$ sintered at 1400°C in air. The inset shows the magnification of $Sr_{1.01}Ti_{0.98}Nb_{0.02}O_{3-\delta}$ XRD pattern at about 2θ=30[deg] in order to expose the impurity phase identified as Sr_2NbO_4

Table 1 Cell parameter of the $SrTi_{1-x}Nb_xO_{3-\delta}$ ($0<x<0.08$) samples sintered at 1400°C in air and reduced at 1400°C in hydrogen.

	Sample sintered at 1400°C in air	Sample sintered at 1400°C in H_2
Composition	cell parameter a/Å	cell parameter a/Å
$SrTiO_{3-\delta}$	3.9055	3.9063
$SrTi_{0.99}Nb_{0.01}O_{3-\delta}$	3.9078	3.9108
$SrTi_{0.98}Nb_{0.02}O_{3-\delta}$	3.9088	
$SrTi_{0.97}Nb_{0.03}O_{3-\delta}$	3.9066	
$SrTi_{0.92}Nb_{0.08}O_{3-\delta}$	3.9063	3.9127
$Sr_{1.01}Ti_{0.98}Nb_{0.02}O_{3-\delta}$	3.9051	

concentration the ($^x/_2$)SrO phase produced in the reaction (1) is completely reacted according to Eqs. (2), (3).

Hashimoto suggests [8] that reactions (2) and (3) take place even in air. The presence of Ti^{3+} and Nb^{4+} products of (2) and (3) reactions, as a result of their ionic radius, cause the increase of unit cell parameter. For higher concentration of niobium dopants the ($^x/_2$)SrO phase produced in the reaction (1) is not completely reacted in reactions (2) and (3) and is partially used to create the Sr_2NbO_4 phase. That is why some impurity phases are observed in the samples with high Nb content. Moreover, formation of the Sr_2NbO_4 leads to a decrease of the amount of Nb in the prerovskite structure as well as to a decrease of concentration of Ti^{3+} and Nb^{4+} products of (2) and (3) reactions. In consequence the unit cell parameter of the perovskite decreases. To further confirm this hypothesis, a sample rich in SrO phase ($Sr_{1.01}Ti_{0.98}Nb_{0.02}O_{3-\delta}$) was prepared. As shown in Fig. 1, the Sr_2NbO_4 phase was observed in this sample. Moreover, the perovskite unit cell parameter of this sample was smaller in comparison with these of the samples with no additional strontium (Table 1). The above results correlate well with our expectations.

The results of electrical conductivity measurement of $SrTi_{0.98}Nb_{0.02}O_{3-\delta}$ reduced in hydrogen at 1200°C, 1300°C and 1400°C for 20 h are shown in Fig. 2. It can be seen that with the increase of reduction temperature, the electrical conductivity increases. Moreover, depending on the reduction temperature, the samples show different types of temperature dependence of conductivity. For samples reduced at 1200°C, a thermally activated behavior is observed in the whole studied temperature range. In the case of the samples reduced at 1300°C and 1400°C, a transition from thermally activated to a metallic-type behavior takes place at some temperature. According to Li et. al. [25] in the temperature range in which the increase of electrical conductivity with temperature is observed, a polaron-type conduction mechanism occurs. That is, the localized electrons hop between the Ti^{3+}, Nb^{4+} and the Ti^{4+}, Nb^{5+} sites. At the critical temperature, the electrons become delocalized and the metallic-type conduction mechanism starts to be significant. The further increase of temperature leads to the decrease of electron mobility and, and as a result, to the decrease of the conductivity.

On the other hand, Irvine [24] and Moss [15, 26] explain such a deviation from the linearity in the conductivity vs. temperature plot by the grain boundary effects. At low temperatures the acceptor-type states located at the grain boundaries create high-ohmic depletion layers. With the increase of temperature, the resistance of that layer decreases and the increase of conductivity is observed. At some temperature this phenomenon can be neglected and the typical metallic-type behaviour starts to dominate.

Figure 3 presents values of electrical conductivity at 600°C, 700°C and 800°C as a function of Nb-content for samples reduced at 1400°C for 20 h. It can be seen that for temperature range 600°C–800°C, the electrical conductivity reaches a maximum in the case of the samples containing 0.02 molar content of Nb. This maximum of conductivity is correlated with the maximum of unit cell parameter. It means that the conductivity value is correlated with the presence of the highest amount of $Ti^{3+}$and Nb^{4+} ions in the structure. These ions become a source of charge carriers, as

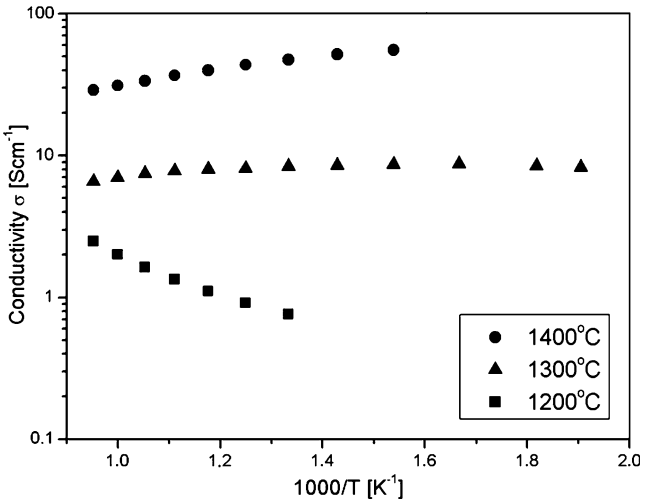

Fig. 2 Electrical conductivity of the $SrTi_{0.98}Nb_{0.02}O_{3-\delta}$ samples reduced in hydrogen at various temperatures for 20 h as a function of temperature

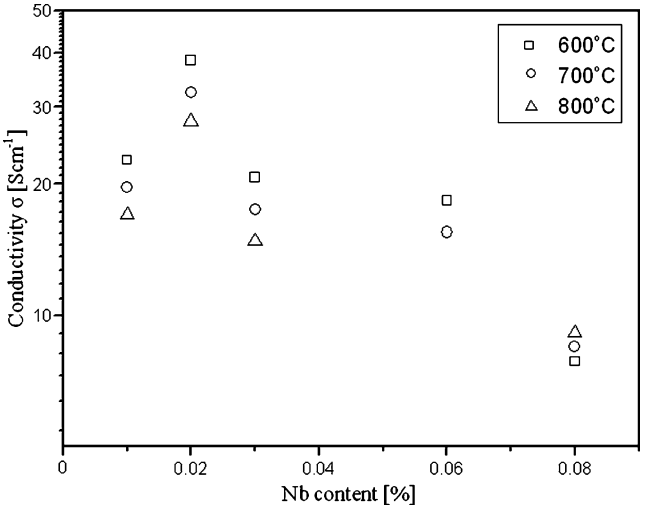

Fig. 3 The values of conductivity at 600°C, 700°C and 800°C of $SrTi_{1-x}Nb_xO_{3-\delta}$ as a function of Nb-content in dry hydrogen, at various temperature. Samples were reduced in hydrogen at 1400°C for 20 h

suggested by Slater et al. [27]. Further doping with increasing Nb amount leads to a gradual decrease of conductivity. This behavior is quite different from that observed in case of strontium titanate doped with yttrium [9, 17] or lanthanum [26, 28], where increasing amount of the dopant leads to increasing conductivity in the whole range of the dopant content.

Conductivity data measured at 800°C as a function of oxygen pressure are shown in Fig. 4. Each data point was obtained after holding the sample in equilibrium conditions for more than 5 h. The data obtained at low and high pressures of oxygen differ slightly. At high oxygen partial pressure, the conductivity remains almost constant, and at low oxygen partial pressure, the value of conductivity is increasing. The existence of such a plateau region correlates well with some previously reported results [15, 18, 22]. In this region the charge carrier concentration depends only on the donor concentration.

In order to use a material as an anode in SOFC it is necessary to obtain about 30% of porosity. Figure 5 presents results of electrical conductivity plotted as a function of temperature for samples with various porosities. Electrical properties of Nb-doped strontium titanate strongly depend on the porosity of samples. For instance, porosity of about 30% causes a decrease of conductivity more than of one order of magnitude. Moreover, it is interesting that the temperature dependence of conductivity of porous samples is weaker than the dependence of the dense one. It suggests a strong influence of grain boundaries on the conductivity mechanism. In order to solve the problem of the deterioration of the electrical conductivity in the porous samples, the knowledge of the relation between the perovskite microstructure and its electrical properties should be deepened. Further studies are in progress.

4 Conclusions

Niobium-doped $SrTiO_3$ samples with various Ti/Nb-ratios were synthesized by a solid-state reaction. The $SrTi_{1-x}Nb_xO_{3-\delta}$ samples with x up to 0.03 show single cubic perovskite structure and no impurity phases were detected. The electrical conductivity of strontium titanate is remarkably enhanced by niobium doping. The highest conductivity was found for the $SrTi_{0.98}Nb_{0.02}O_{3-\delta}$ sample. This maximum of conductivity is correlated with the maximum of the unit cell parameter. Both of these effects are caused

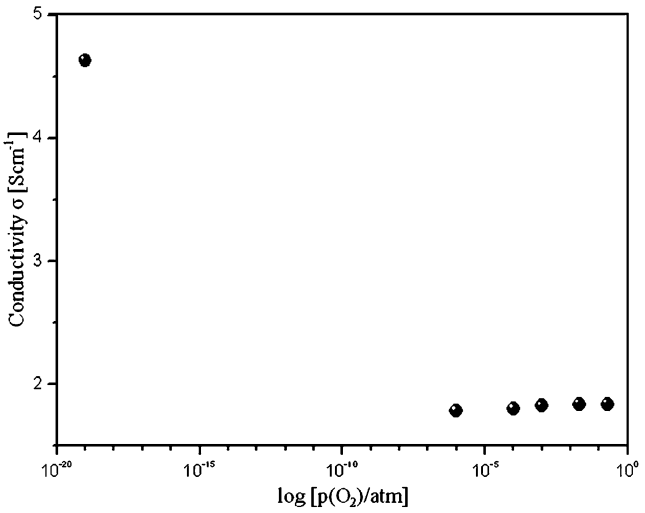

Fig. 4 Conductivity of $SrTi_{0.98}Nb_{0.02}O_{3-\delta}$ at 800°C as a function of oxygen partial pressure. Samples were reduced in hydrogen at 1400°C for 20 h

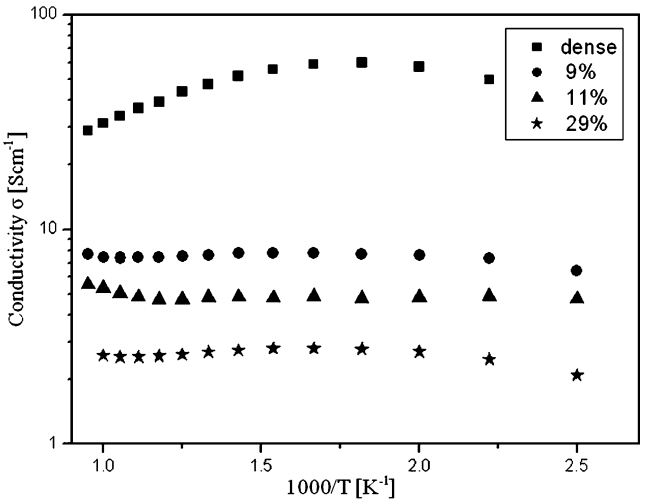

Fig. 5 Temperature dependence of electrical conductivity of the $SrTi_{0.98}Nb_{0.02}O_{3-\delta}$ samples with various porosity. Samples were reduced in hydrogen at 1400°C for 20 h

by the amount of $Ti^{3+}$and Nb^{4+} ions. It was shown that the temperature of reduction and the porosity of samples could significantly change electrical properties of $SrTi_{1-x}Nb_xO_{3-\delta}$. Despite that, even for samples with the porosity of about 30%, which is necessary for SOFC anode application, the conductivity level is sufficient. In conclusion, the presented results make the Nb-doped strontium titanate an interesting material for further investigations as a new SOFC anode material.

Acknowledgment This work is supported by the project MNiSW N511 005 31/05/76.

References

1. J.W. Fergus, Solid State Ion. **177**, 1529–1541 (2006). doi:10.1016/j.ssi.2006.07.012
2. K.C. Wincewicz, J.S. Cooper, J. Power Sources **140**, 280–296 (2005). doi:10.1016/j.jpowsour.2004.08.032
3. A. Atkinson, S. Barnett, R.J. Gorte, J.T.S. Irvine, A.J. Mcevoy, M. Mogensen, S.C. Singhal, J. Vohs, Nature **3**, 17–27 (2004). doi:10.1038/nmat1040
4. C. Sun, U. Stimming, J. Power Sources **171**, 247–260 (2007). doi:10.1016/j.jpowsour.2007.06.086
5. A. Rachel, S.G. Ebbinghaus, M. Güngerich, P.J. Klar, J. Hanss, A. Weidenkaff, A. Reller, Thermochim. Acta **438**, 134–143 (2005). doi:10.1016/j.tca.2005.08.010
6. S. Tao, J.T.S. Irvine, Chem. Rec. **4**, 83–95 (2004). doi:10.1002/tcr.20003
7. H. Kurokawa, L. Yang, C.P. Jacobson, L.C. De Jonghe, S.J. Visco, J. Power Sources **164**, 510–518 (2007). doi:10.1016/j.jpowsour.2006.11.048
8. S. Hashimoto, F.W. Poulsen, M. Mogensen, J. Alloy. Comp. **439**, 232–236 (2007). doi:10.1016/j.jallcom.2006.05.138
9. Q.X. Fu, S.B. Mi, E. Wessel, F. Tietz, J. Eur. Ceram. Soc. **28**, 811–820 (2008). doi:10.1016/j.jeurceramsoc.2007.07.022
10. S.Q. Hui, A. Petric, J. Electrochem. Soc. **149**, J1–J10 (2002). doi:10.1149/1.1420706
11. U. Balachandran, N.G. Eror, J. Electrochem. Soc. **129**, 1021–1026 (1982)
12. O. Odekirk, U. Balachandran, N.G. Eror, J.S. Blakemore, J. Am. Cer. Soc. **66**, C22–C23 (1983)
13. U. Balachandran, N.G. Eror, J. Am. Cer. Soc. **64**, C75–C76 (1981)
14. N.G. Eror, U. Balachandran, J. Solid. State Chem. **40**, 85–91 (1981)
15. R. Moos, S. Schollhammer, K.H. Härdtl, Appl. Phys. A. **65**, 291–294 (1997). doi:10.1007/s003390050581
16. T. Kolodiazhnyi, A. Petric, J. Electroceramics **15**, 5–11 (2005)
17. H. Zhao, F. Gao, X. Li, C. Zhang, Z. Zhao, Solid State Ionics **180**, 193–197 (2009)
18. P. Blennow, A. Hagen, K.K. Hansen et al., Solid State Ionics **179**, 2047–205 (2008)
19. J. Karczewski, B. Riegel, S. Molin, A. Winiarski, M. Gazda, P. Jasinski, L. Murawski, B. Kusz, J. Alloys Compd. **473**, 496–499 (2009)
20. P. Blennow, K.K. Hansen, L.R. Wallenberg, M. Mogensen, Solid State Ionics **180**, 63–70 (2009)
21. F. Horikiri, N. Iizawa, L.Q. Han, K. Sato, K. Yashiro, T. Kawada, J. Mizusaki, Solid State Ionics **179**, 2335–2344 (2008)
22. R. Moos, K.H. Härdtl, J. Am. Ceram. Soc. **80**, 2549–2562 (1997)
23. A.A.L. Ferreira, J.C.C. Abrantes, J.A. Labrincha, J.R. Frade, J. European, Ceramic Society **19**, 773–776 (1999)
24. J.T.S. Irvine, P.R. Slater, P.A. Wright, Ionics **2**, 213–216 (1996)
25. X. Li, H. Zhao, W. Shen, F. Gao, X. Huang, Y. Li, Z. Zhu, J. Power, Sources **166**, 47–52 (2007)
26. R. Moos, K.H. Härdtl, J. Appl. Phys. **80**, 393–400 (1996)
27. P.R. Slater, D.P. Fagg, J.T.S. Irvine, J. Mater. Chem. **7**, 2495–2498 (1997)
28. X. Li, H. Zhao, F. Gao, N. Chen, N. Xu, Electrochem. Commun. **10**, 1567–1570 (2008)